# Recent Development on the Graphene Reinforced Geopolymer Composites

Jingkun Yuan, Peigang He, Dechang Jia

Institute for Advanced Ceramics (IAC)
School of Mater Science and Engineering
Harbin Institute of Technology (HIT), Harbin, China

Saint-Quentin, North of Paris, France
July 10-12, 2017

# Outline

# 1. Introduction

## Geopolymer

- **Empirical formula**

$$M_n\{\text{-}(SiO_2)_z\text{-}AlO_2\}n \cdot wH_2O$$

$M$ - alkali metallic ion;
$n$ - degree of polymerization;
$z$ - Mole ratio of $SiO_2$ to $Al_2O_3$;
$w$ - Water of crystallization.

- **Structure**

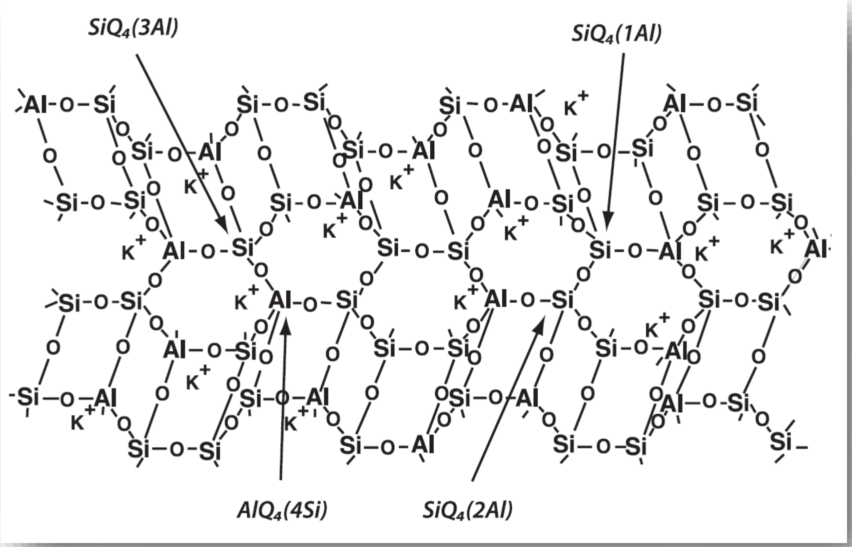


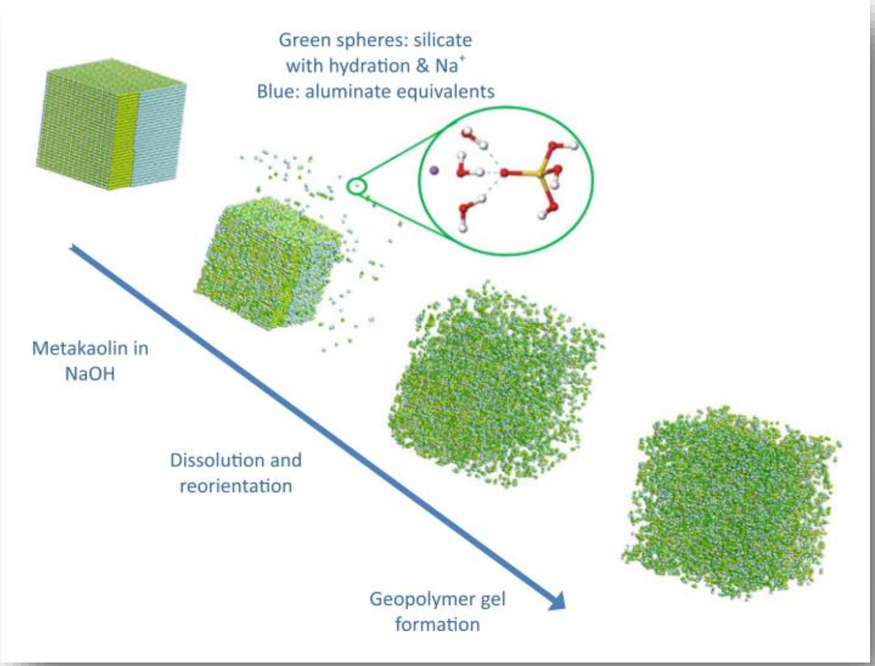


Schematic of the description of metakaolin geopolymerisation by a coarse-grained Monte Carlo model

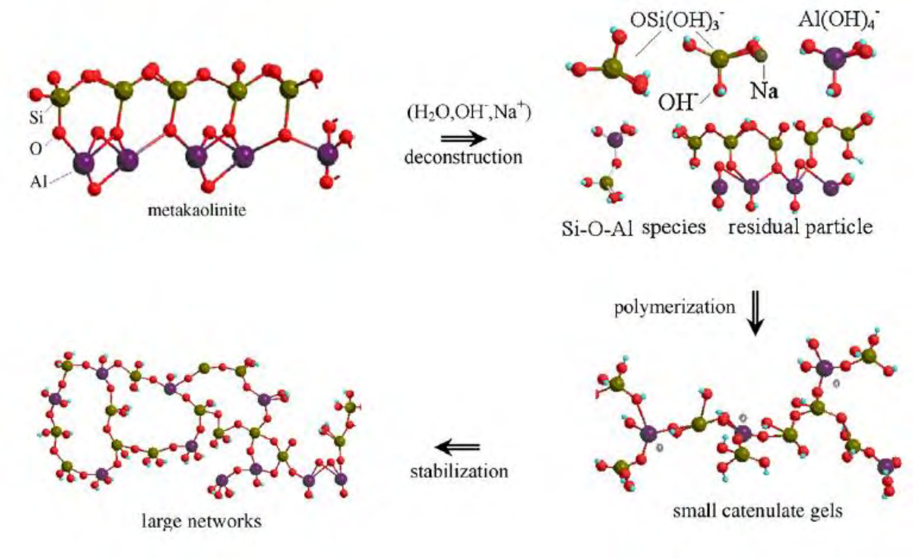


Sketch of the geopolymerization process

# 1. Introduction

## Graphene

- One-atom-thick carbon material, with carbon atoms packed densely in a hexagonal honeycomb lattice.
- A basic building block for graphitic materials of all other dimensionalities.
- It can be wrapped up into 0D fullerenes, rolled into 1D nanotubes or stacked into 3D graphite

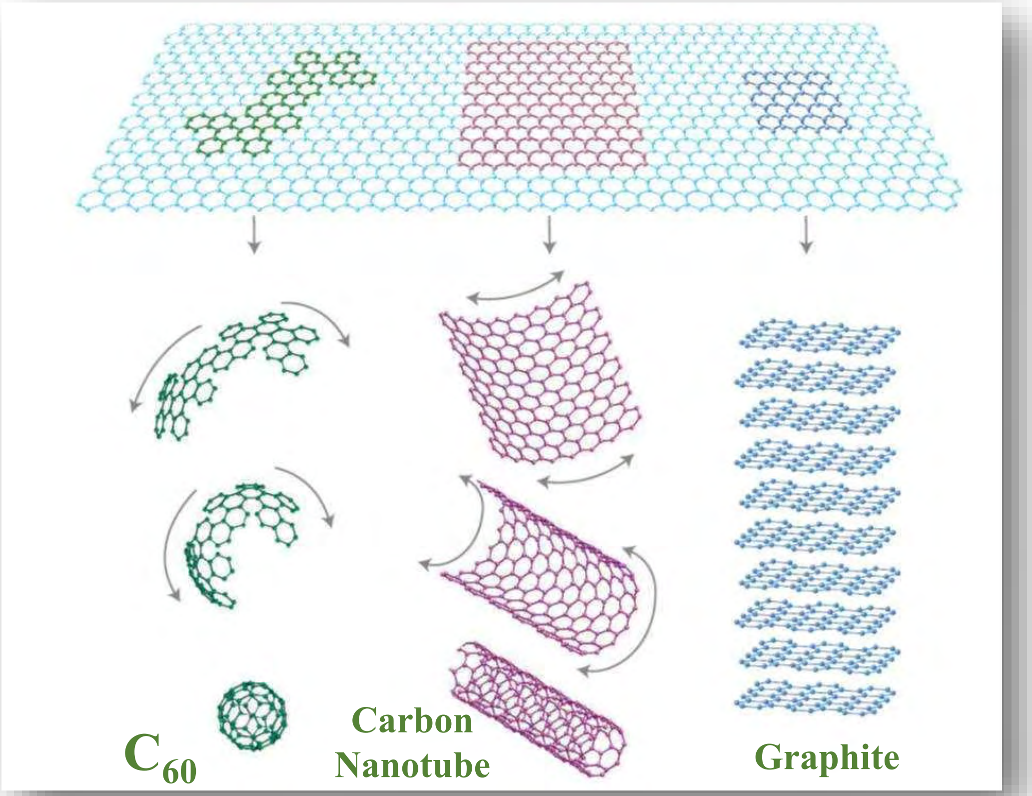


Excellent performance
- Thermal property
- Electrical property
- Mechanical property

Difficult to disperse

## Graphene oxide (GO)

Hydrophily
Easy to disperse

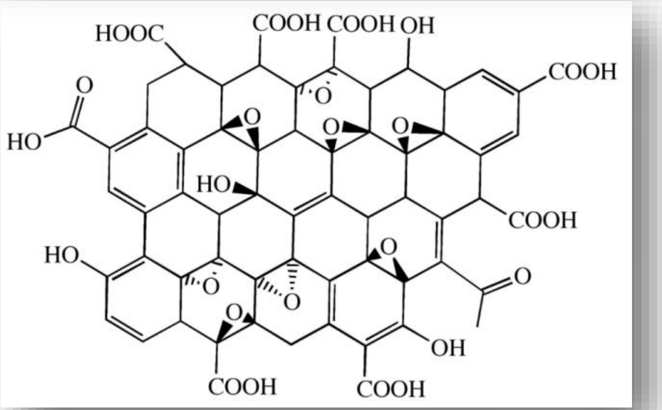

# 1. Introduction

## Graphene oxide (GO)

- ✓ water solubility
- ✓ in-situ reduction:
  - *alkaline reduction*
  - *thermal reduction*

## Geopolymer

- ✓ aqueous environment
- ✓ alkaline environment
- ✓ in-situ convert into advanced ceramics

*in-situ synthesis*

**Graphene/geopolymer composites**

**Graphene/ceramic matrix composites**

*High temperature treatment*

# 2. Preparation process

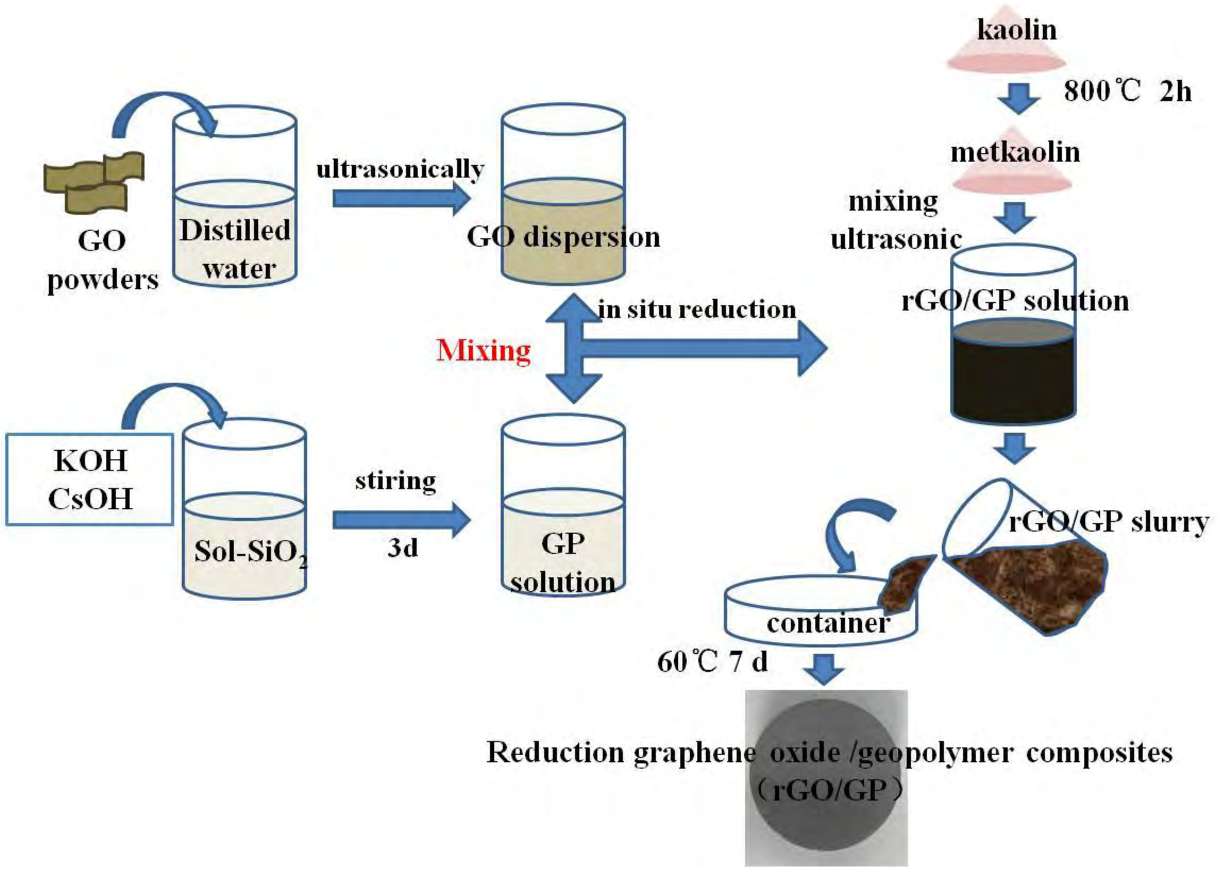


Schematic illustration of preparation procedure for rGO/geopolymer composite

## ● Reduction mechanism

| GO (wt%) | Reduction reaction | |
|---|---|---|
| | Temperature (°C) | Time (h) |
| 1 | RT | 0.5 |
| | 40 | 3 |
| | 60 | 6 |
| | 80 | 72 |

## ● Geopolymerization mechanism

| GO (wt%) | Geopolymerization reaction time (h) |
|---|---|
| 0, 1 | 0, 0.5, 1, 2, 3, 6, 12, 24, 72, 120, 168 |

## ● rGO/Geopolymer Composites

| GO (wt%) |
|---|
| 0, 0.05, 0.1, 0.3, 0.5, 1 |

**reduced graphene oxide (rGO)**

# 3. In situ reduction mechanism

## 3.1 Effects of reduction temperature

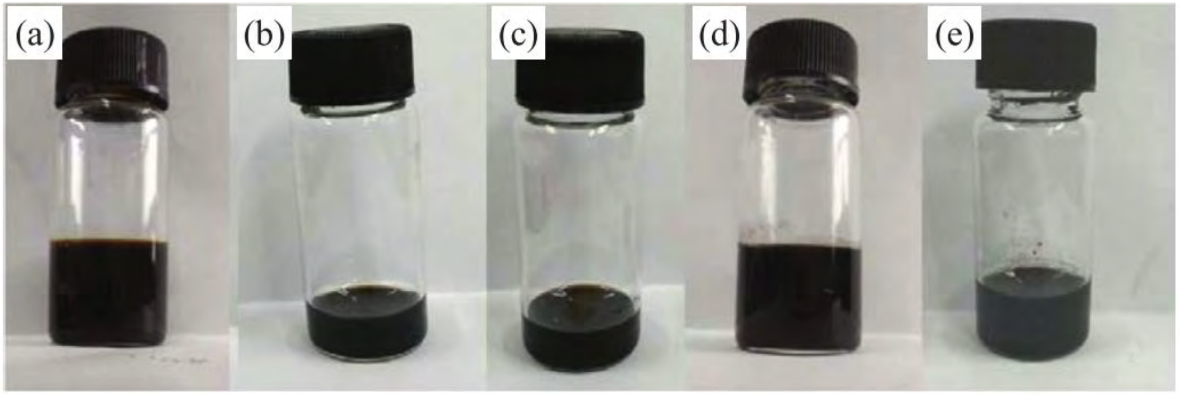


Optical photographs of GO suspension (a) in deionized water and GO after being reduced under alkaline solution at different temperatures: (b)-(e) RT, 40 °C, 60 °C and 80 °C, respectively

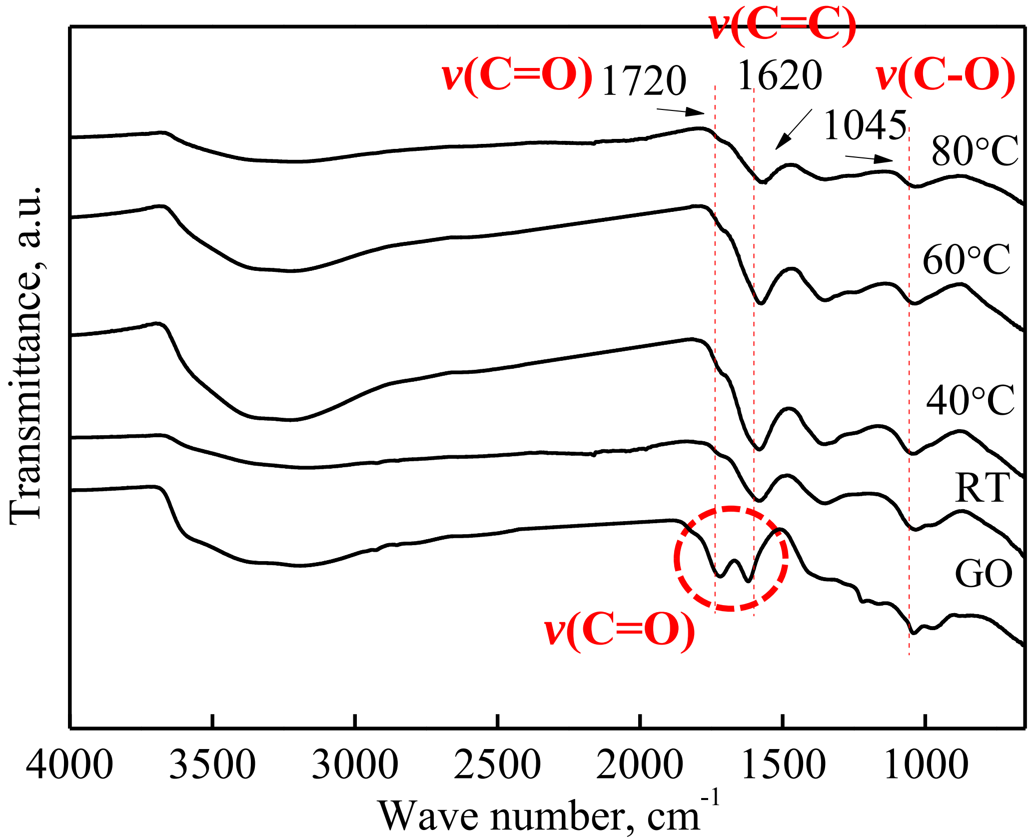


FT-IR spectras of GO and rGO obtained after being reduced under alkaline solution for different temperatures

# 3. In situ reduction mechanism

## 3.1 Effects of reduction temperature

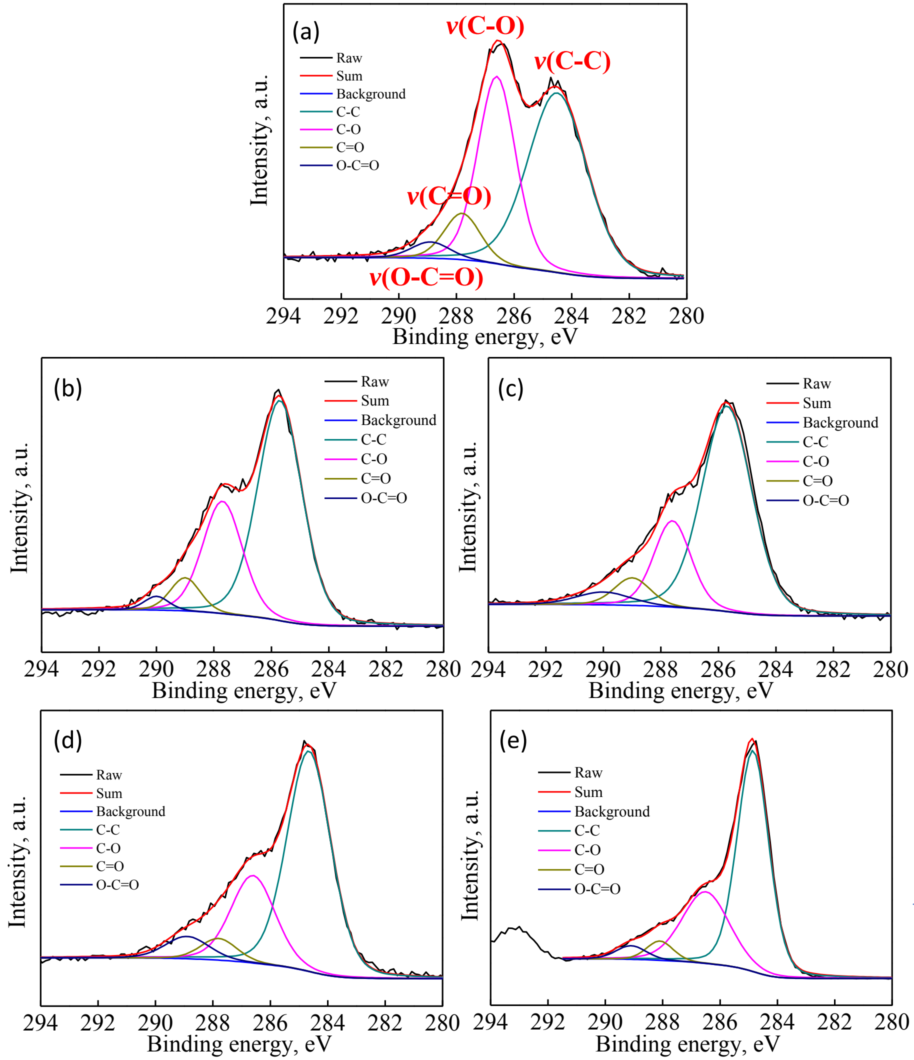


Values of C/O atomic ratios and peak area ratios of oxygen-containing bonds to C-C bonds obtained by XPS analysis of GO and rGO reduced for 3h at different temperatures

| Temperature (°C) | C/O Ratio | C-O | C=O | O-C=O |
|---|---|---|---|---|
| GO | 2.48 | 0.67 | 0.16 | 0.06 |
| RT | 2.74 | 0.5 | 0.1 | 0.03 |
| 40 | 2.85 | 0.31 | 0.1 | 0.07 |
| 60 | 3.06 | 0.4 | 0.08 | 0.1 |
| 80 | 3.36 | 0.48 | 0.07 | 0.06 |

High resolution $C_{1s}$ X-ray photoelectron spectra for GO and rGO reduced for 3h at different temperatures: (a) GO, (b) RT, (c) 40°C, (d) 60°C, (e) 80°C

# 3. In situ reduction mechanism

## 3.1 Effects of reduction temperature

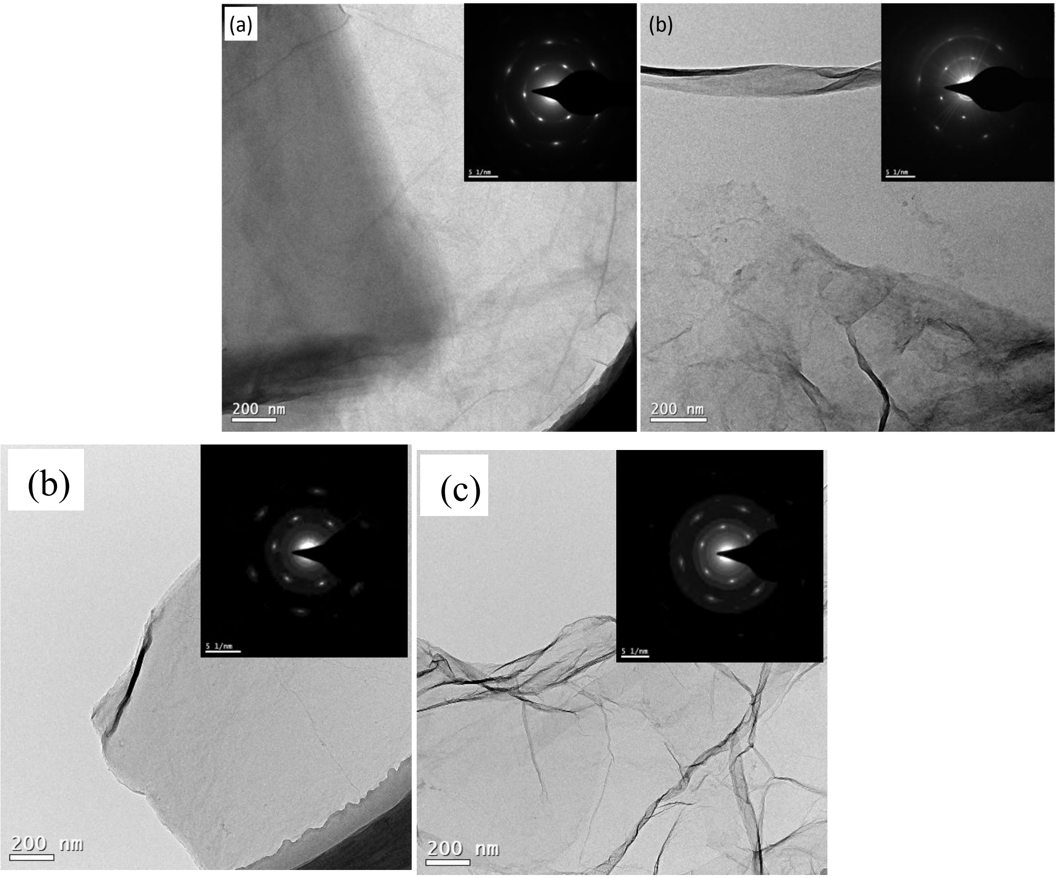


Typical TEM images and selected area electron diffraction (SAED) patterns of rGO reduced at different temperatures: (a) GO, (b) 60$^{o}$C, (e) 80$^{o}$C

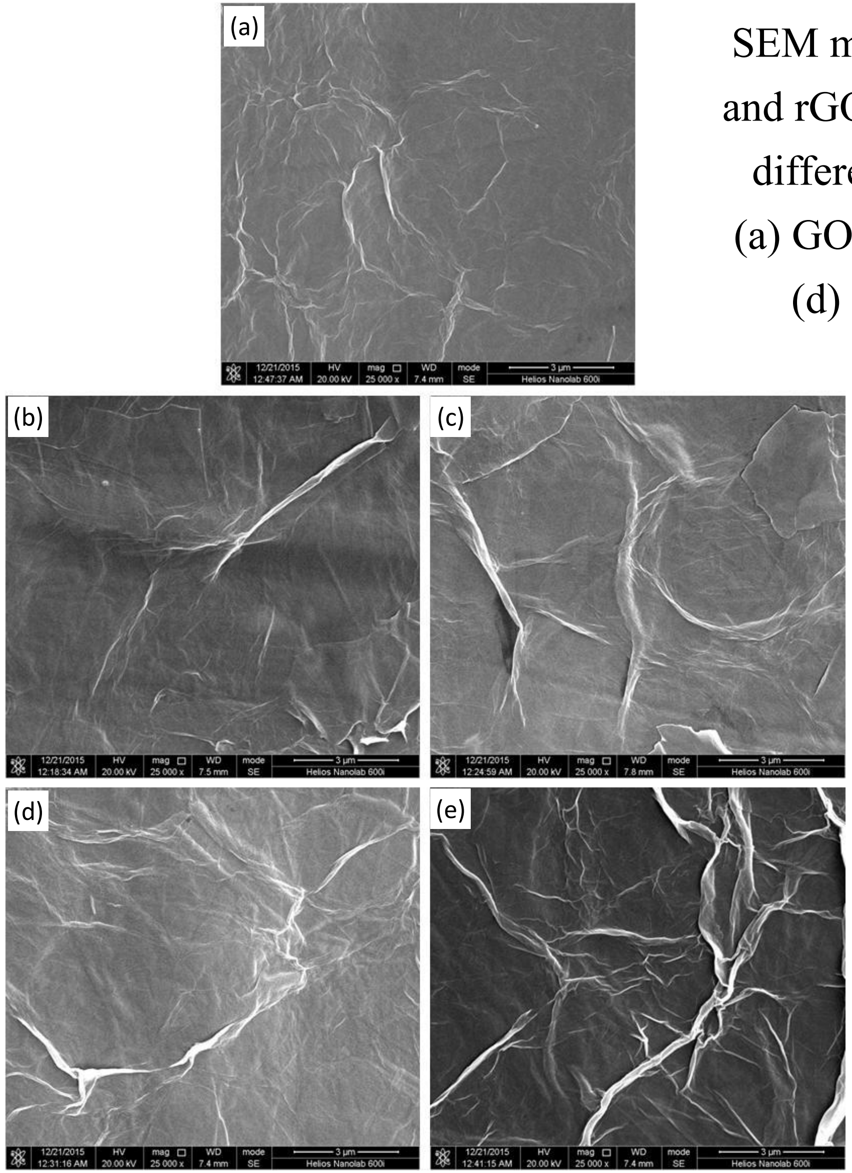


SEM micrographs of GO and rGO reduced for 3h at different temperatures: (a) GO, (b) RT, (c) 40$^{o}$C, (d) 60$^{o}$C, (e) 80$^{o}$C

# 3. In situ reduction mechanism

## 3.2 Effects of reduction time

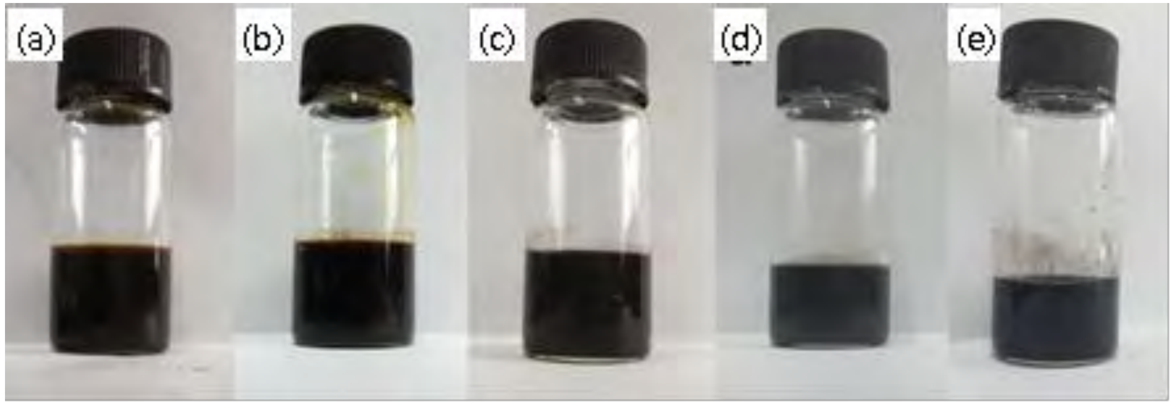


Optical photographs of GO suspension and GO after being reduced under geopolymeric solution at 60°C for different times: (a) GO suspension, (b) 0.25h, (c) 3h, (d) 6h, (e) 72h

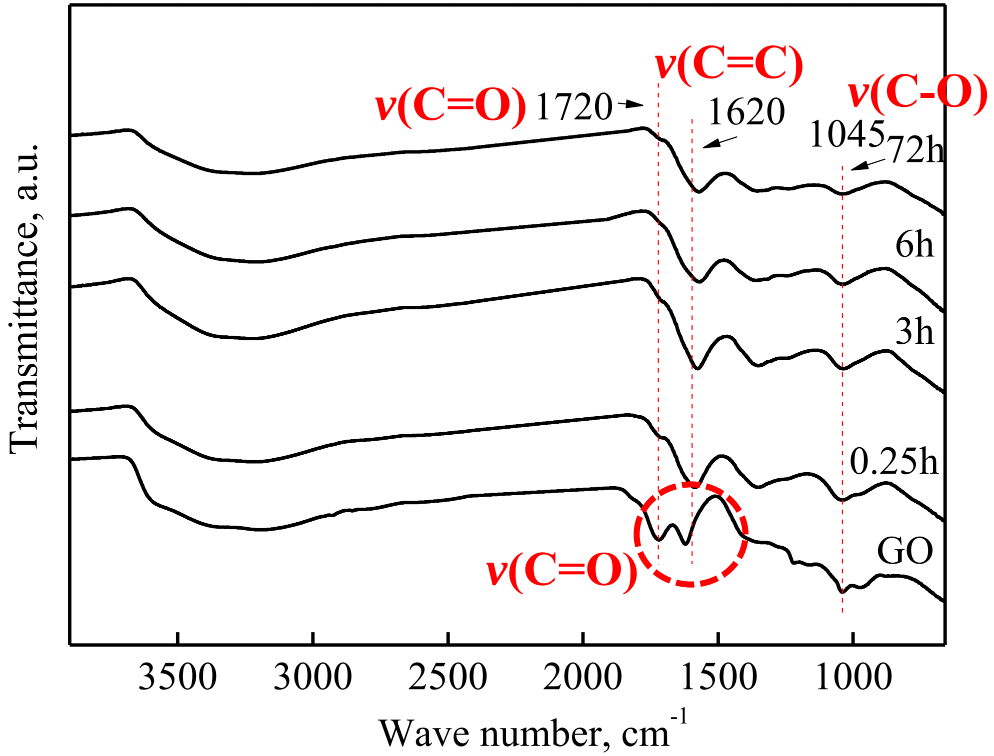


FT-IR spectras of GO and rGO reduced at 60°C at different times

# 3. In situ reduction mechanism

## 3.2 Effects of reduction time

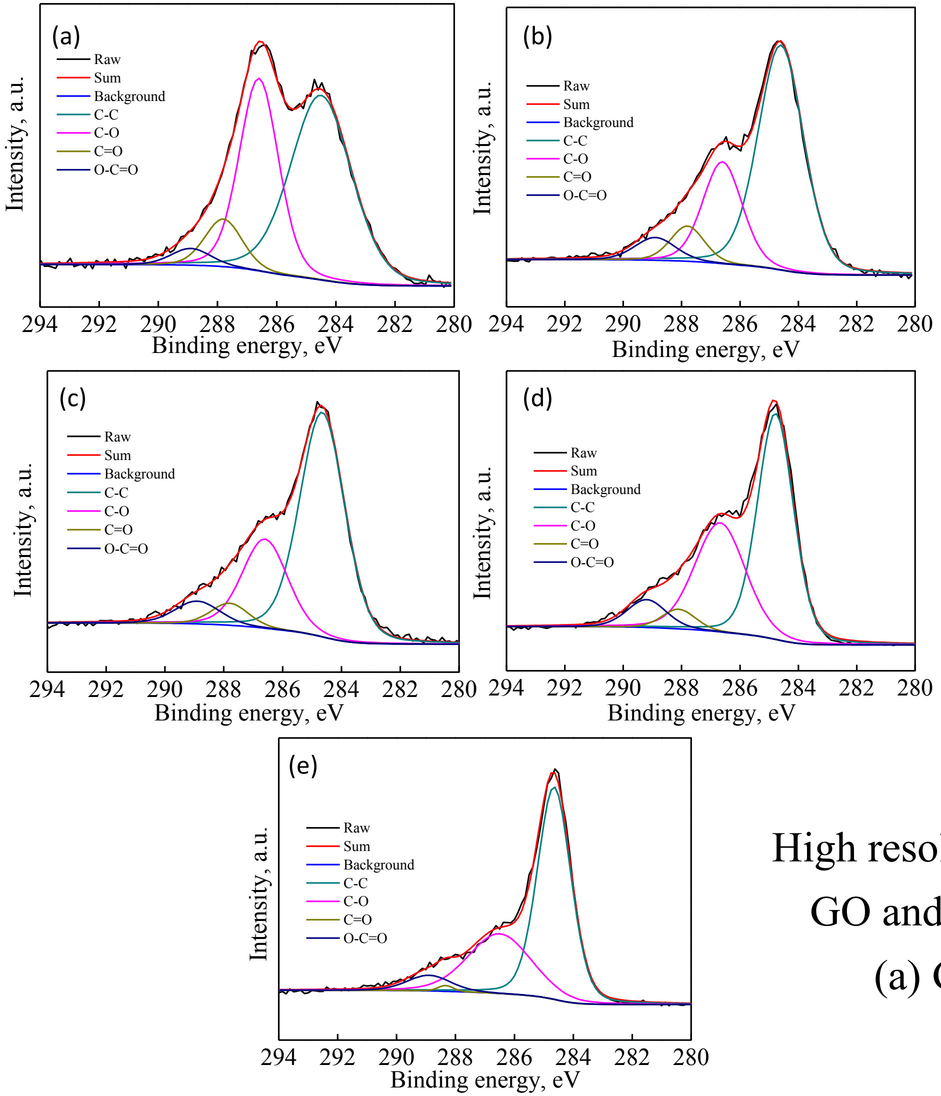


Values of C/O atomic ratios and peak area ratios of oxygen-containing bonds to C-C bonds obtained by XPS analysis of GO and rGO reduced at 60°C for different times

| Samples | C/O Ratio | C-O | C=O | O-C=O |
|---|---|---|---|---|
| GO | 2.48 | 0.67 | 0.16 | 0.06 |
| 0.25h | 3.03 | 0.39 | 0.12 | 0.09 |
| 3h | 3.06 | 0.40 | 0.08 | 0.10 |
| 6h | 3.19 | 0.66 | 0.07 | 0.12 |
| 72h | 3.75 | 0.53 | 0.01 | 0.09 |

$$R\text{-}COOH + KOH \rightarrow RH + K_2CO_3 + H_2O$$

High resolution C1s X-ray photoelectron spectra for GO and rGO reduced at 60°C at different times:
(a) GO, (b) 0.25h, (c) 3h, (d) 6h, (e) 72h

# 3. In situ reduction mechanism

## 3.2 Effects of reduction temperature

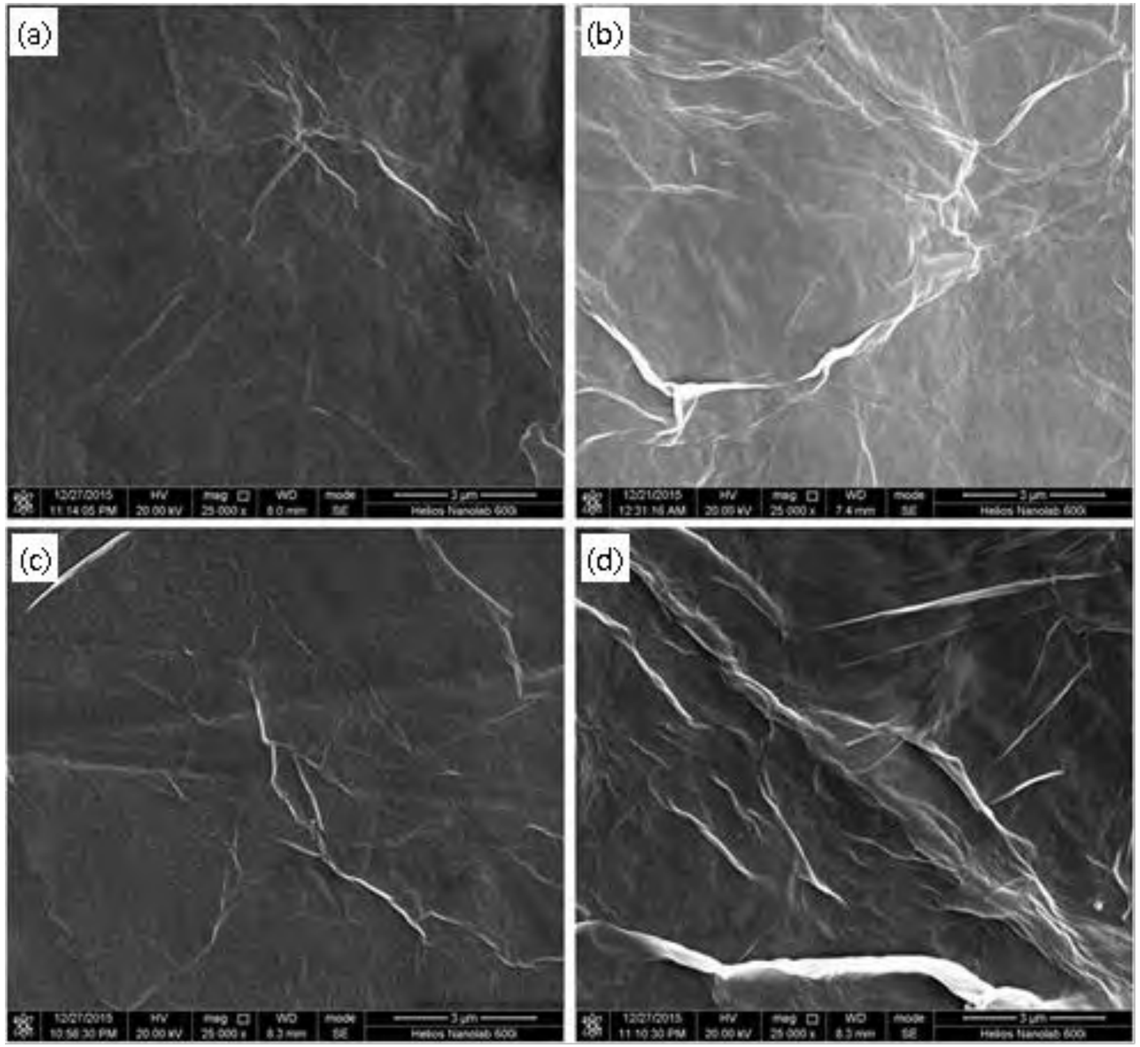


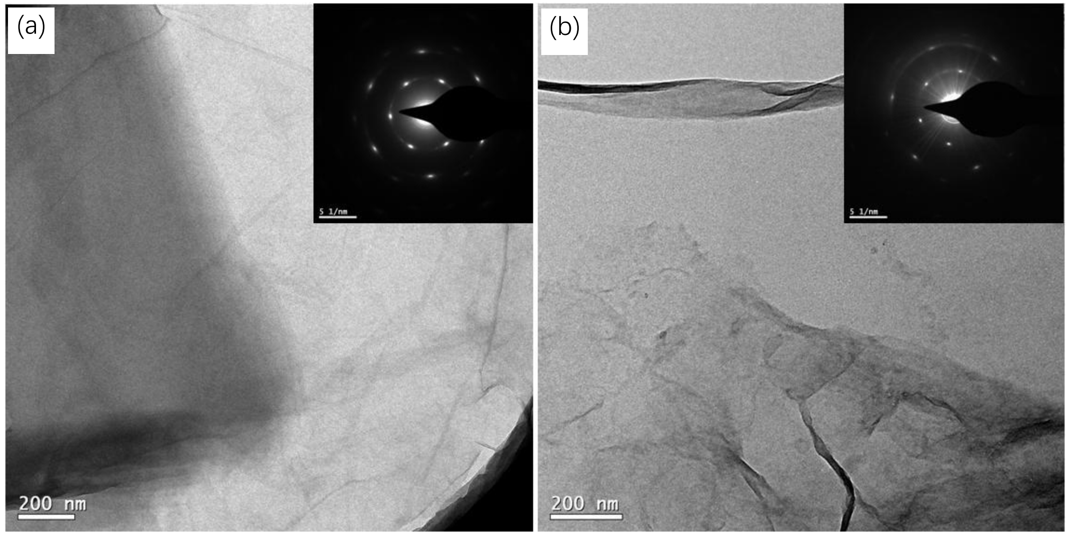


Typical TEM images and the selected area electron differention (SAED) patterns (insets at upper right corner)of GO and rGO: (a) GO, (b) rGO for 72 h

SEM micrographs of rGO reduced at 60$^o$Cfor different times: a) 0.25 h, (b) 3 h, (c) 6 h, (d) 72 h

# 3. In situ reduction mechanism

$$GO \rightarrow rGO + CO_2 + CO + H_2O$$

## 3.3 Thermal reduction

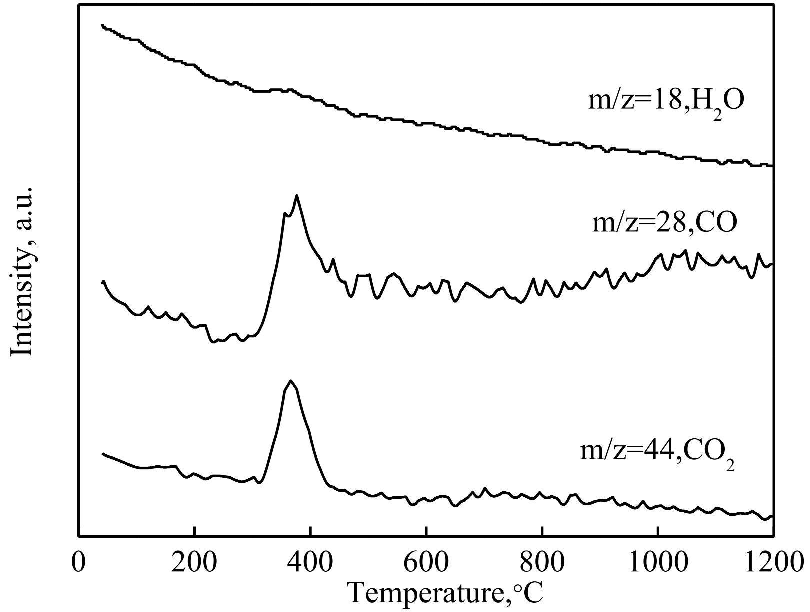


MS analysis of GO in argon atmosphere

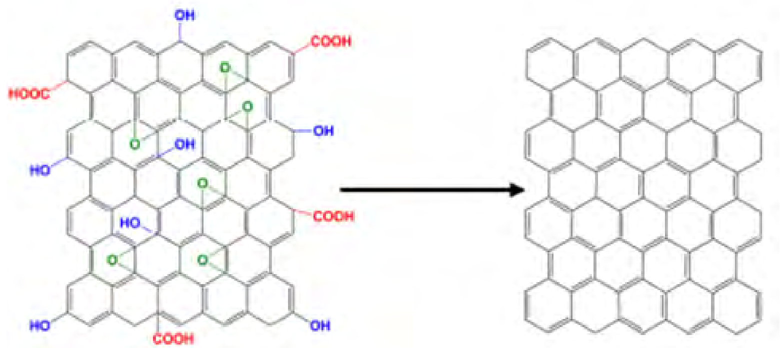


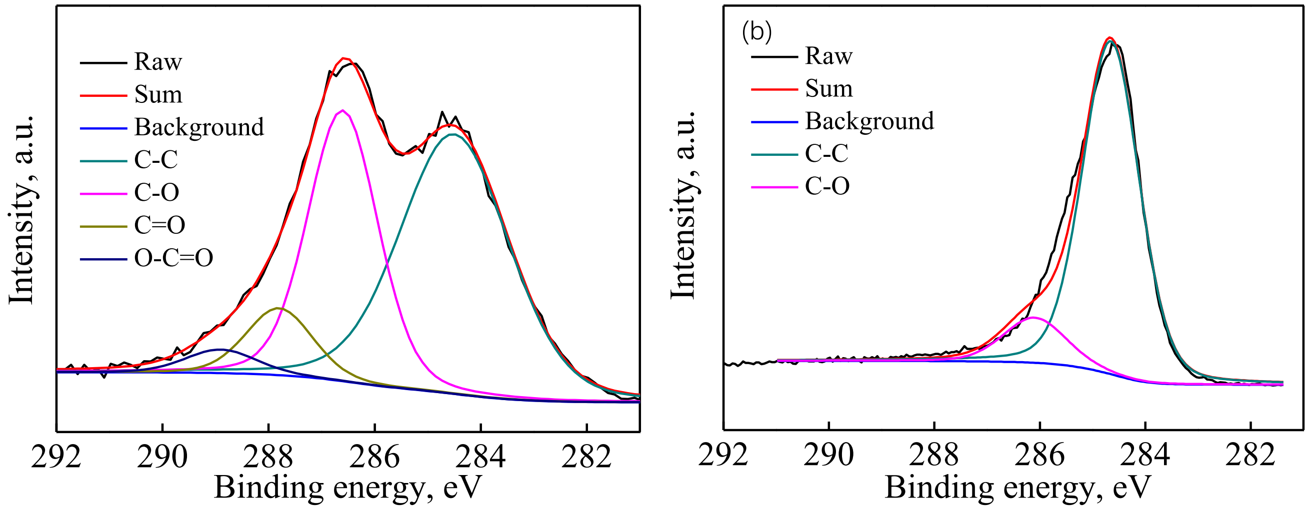


High resolution C1s X-ray photoelectron spectra of GO and rGO obtained after high temperature treatment at 1000°C for 0.5h: (a) GO, (b) rGO

Peak area ratios of C-C bond and oxygen-containing bonds obtained by XPS analysis of GO and rGO

| Bond | C-C | C-O | C=O | O-C=O |
|---|---|---|---|---|
| GO | 0.53 | 0.36 | 0.08 | 0.03 |
| rGO | 0.87 | 0.13 | -- | -- |

# 3. In situ reduction mechanism

**Alkaline reduction： decarboxylic reaction**

**R-COOH+KOH→RH+$K_2CO_3$+$H_2O$**

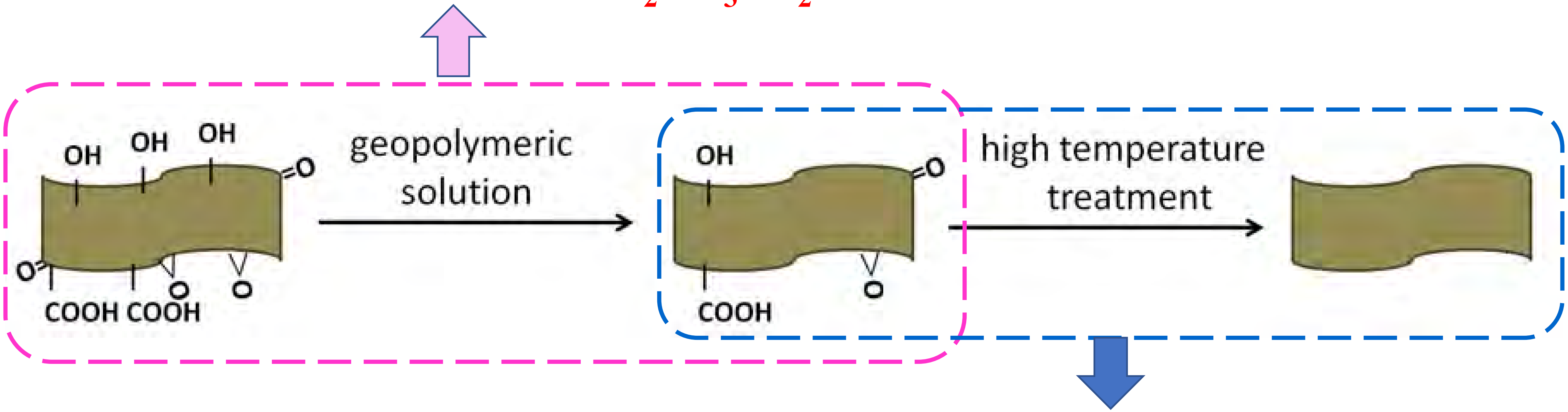


**Thermo reduction：**

**GO→rGO+CO+$H_2O$+$CO_2$**

# 4. rGO/geopolymer composites (rGO/KGP)

## 4.1 Phase composition

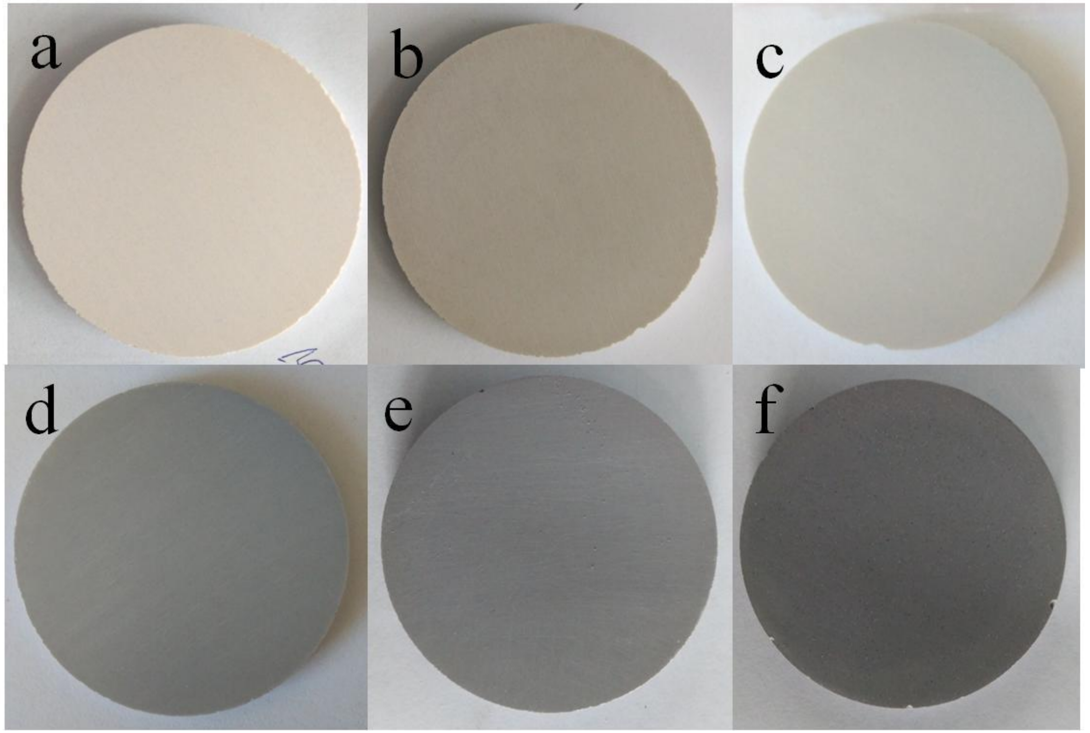


The photographs of rGO/KGP composites with different rGO contents (wt%), (a) 0, (b) 0.05, (c) 0.1, (d) 0.3, (e) 0.5 and (f) 1

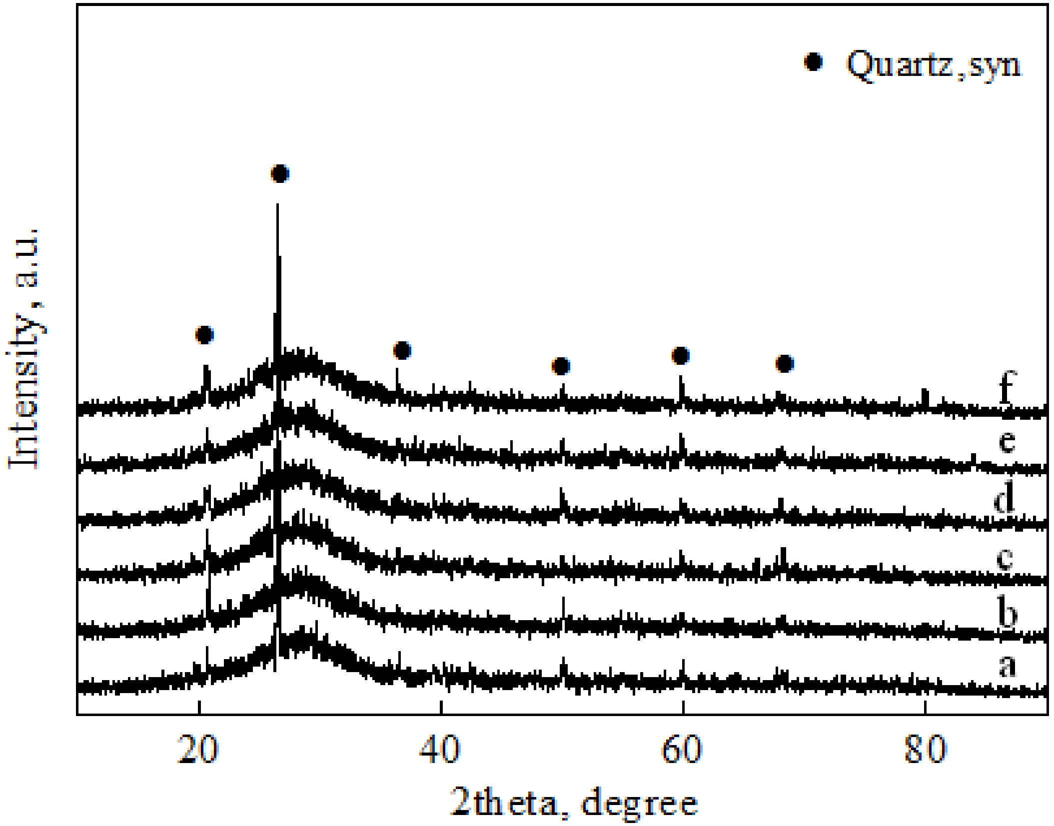


XRD patterns of rGO/KGP composites with different rGO contents(wt%), (a) 0, (b) 0.05, (c) 0.1, (d) 0.3, (e) 0.5 and (f) 1

# 4. rGO/geopolymer composites (rGO/KGP)

## 4.2 Microstructure

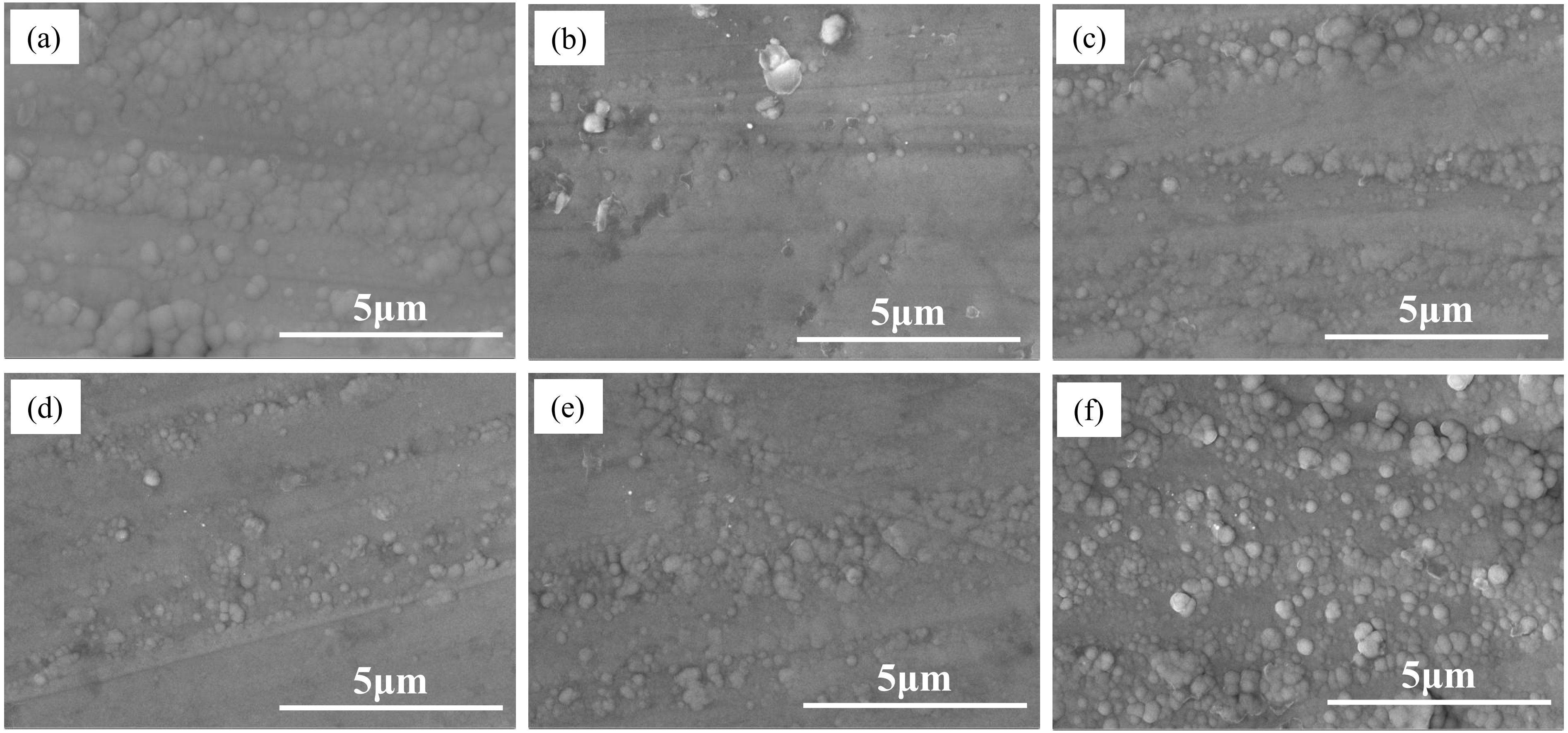


Typical surface microstructure of rGO/KGP composites with different GO contents:
(a) 0wt.%, (b) 0.05wt.%, (c) 0.1wt.%, (d) 0.3wt.%, (e) 0.5wt.%, (f) 1wt.%

# 4. rGO/geopolymer composites (rGO/KGP)

## 4.4 Fracture morphology

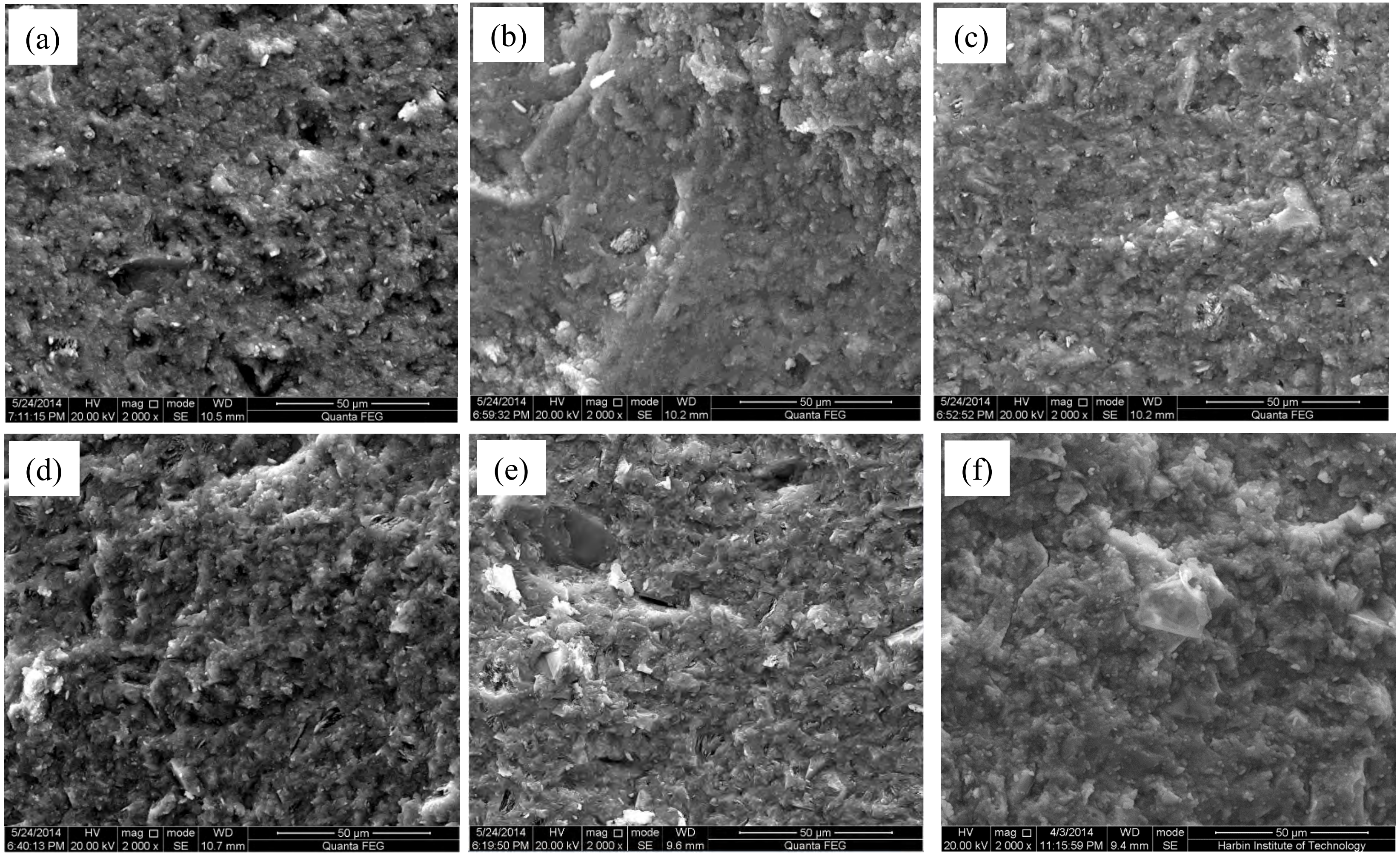


Fracture morphologyof rGO/KGP with different GO contents: (a) 0wt.%, (b) 0.05wt.%, (c) 0.1wt.%, (d) 0.3wt.%, (e) 0.5wt.%, (f) 1wt.%

# 4. rGO/geopolymer composites (rGO/KGP)

## 4.4 Fracture morphology

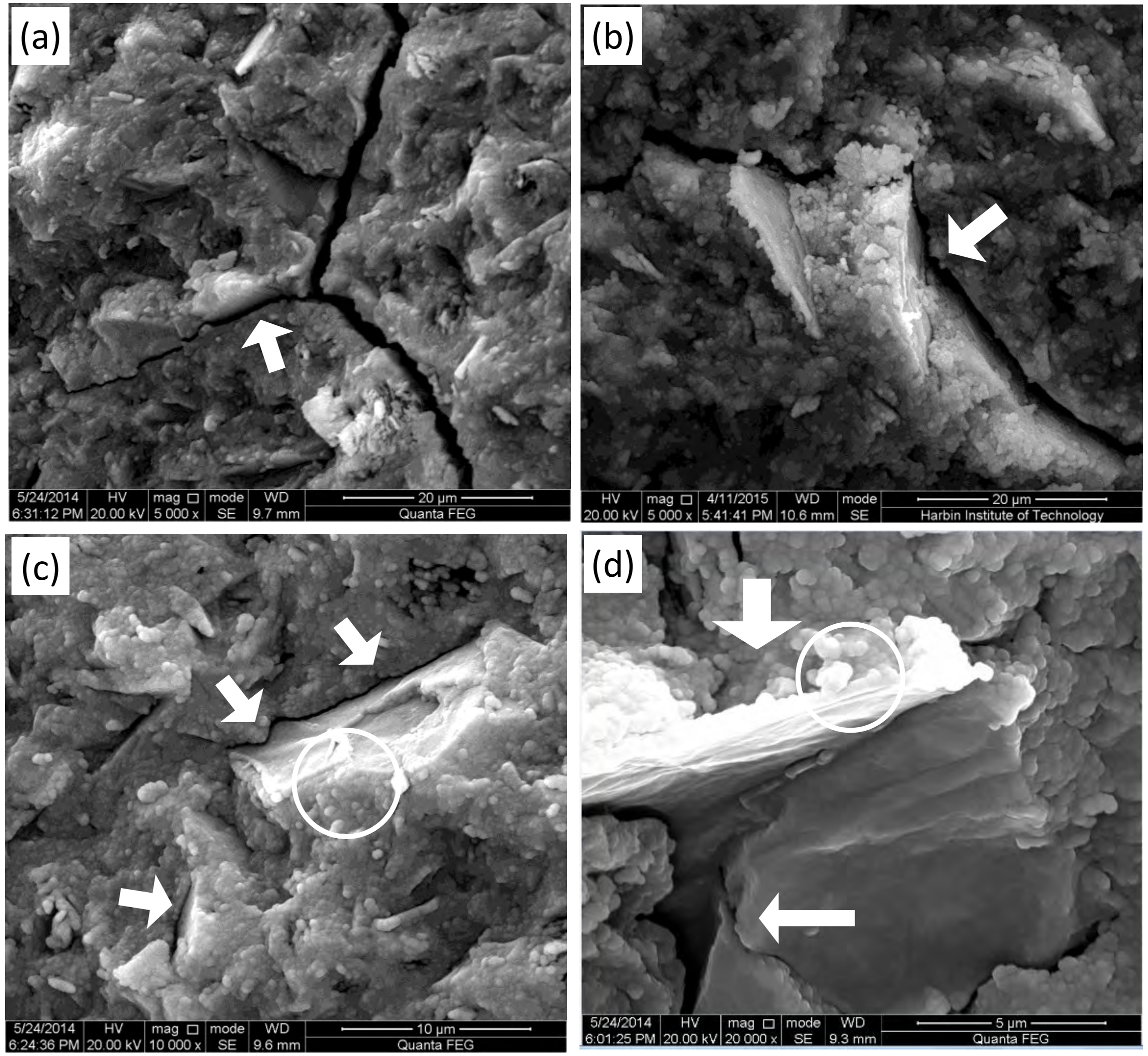


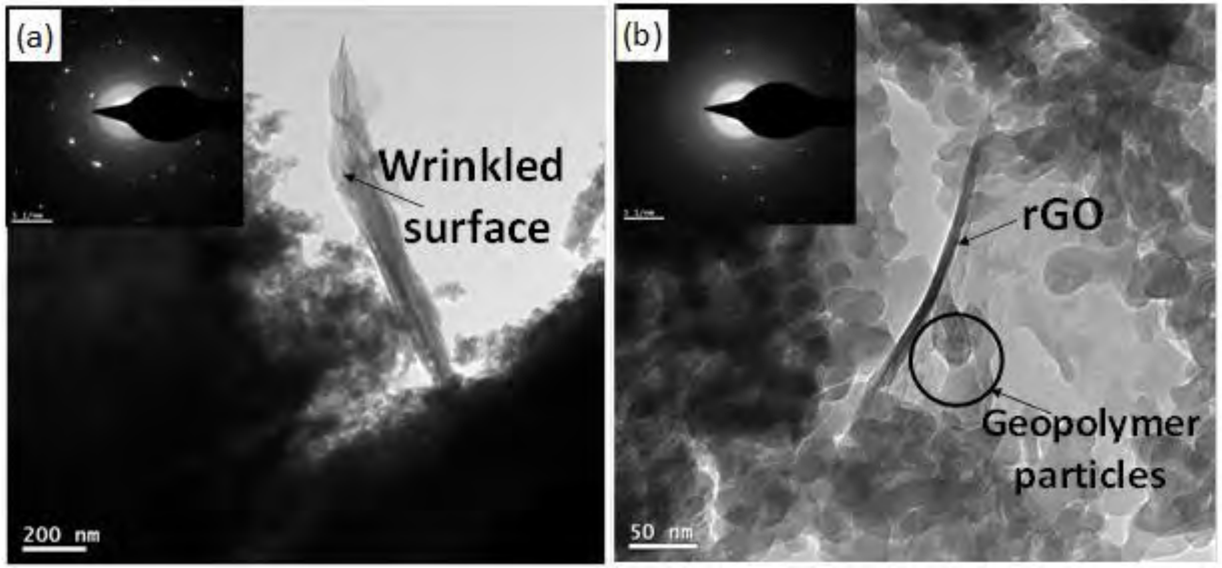


TEM images of rGO/KGP5, insets display selected electronic diffraction patterns: (a)wrinkled rGO with matrix, (b) bonding between rGO and matrix

Detailed observation of interface microstructure of the rGO/KGP5 composites: (a)-(b) deflected crack, (c) bonding between KGP and rGO, (d) rGO pulling out

# 4. rGO/geopolymer composites (rGO/KGP)

## 4.1 Phase composition

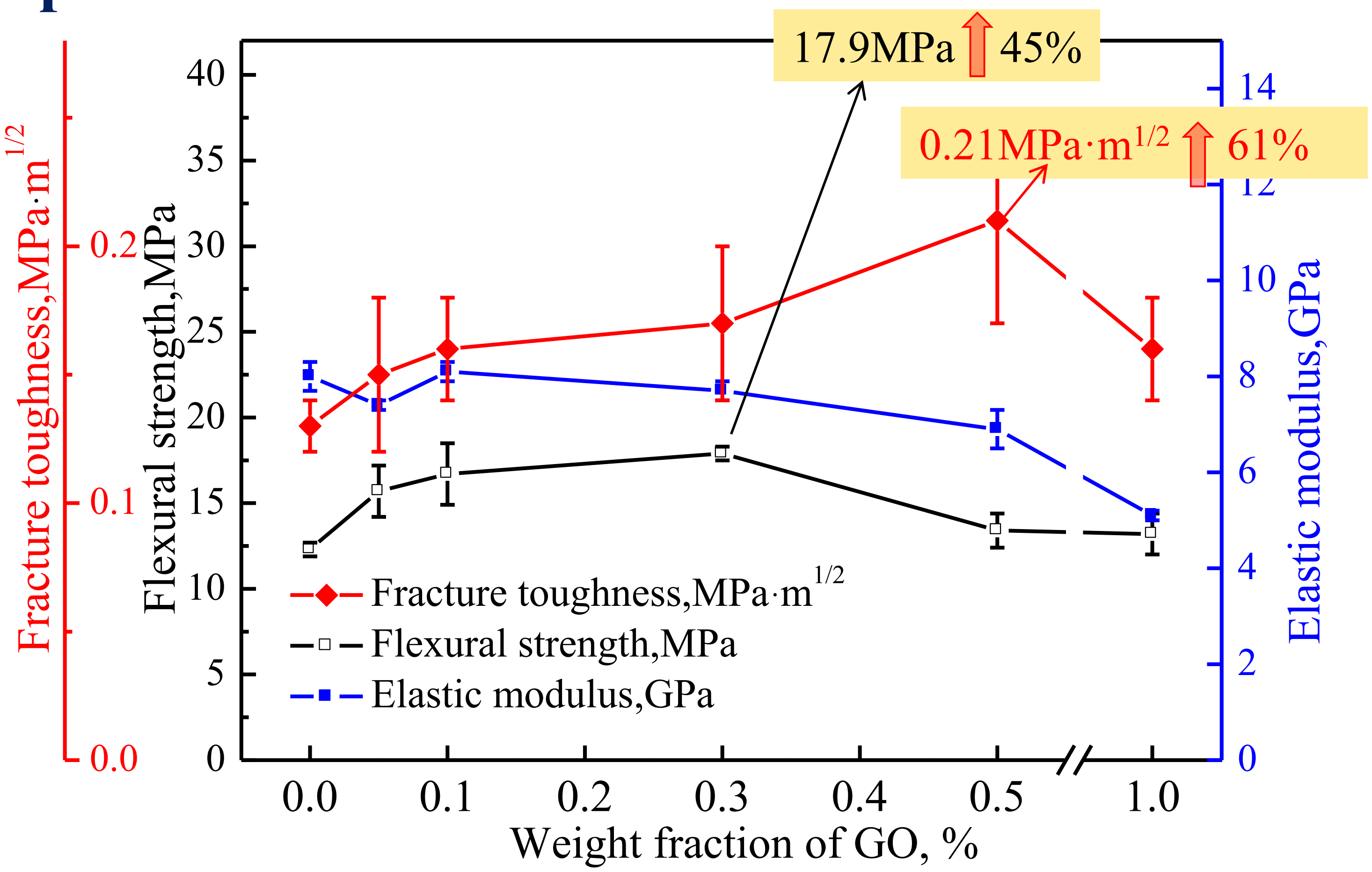


Mechanical properties of rGO/KGP composites with different GO contents

# 5. Thermal evolution of rGO/KGP

## 5.1 Crystallization kinetics

$$\frac{dx}{dt} = K(1-x)^n$$

$$K = K_0 \exp\left[-\frac{E}{RT}\right]$$

$$\ln\left(\frac{\beta}{T_p^2}\right) = -\frac{E}{RT_p} + C$$

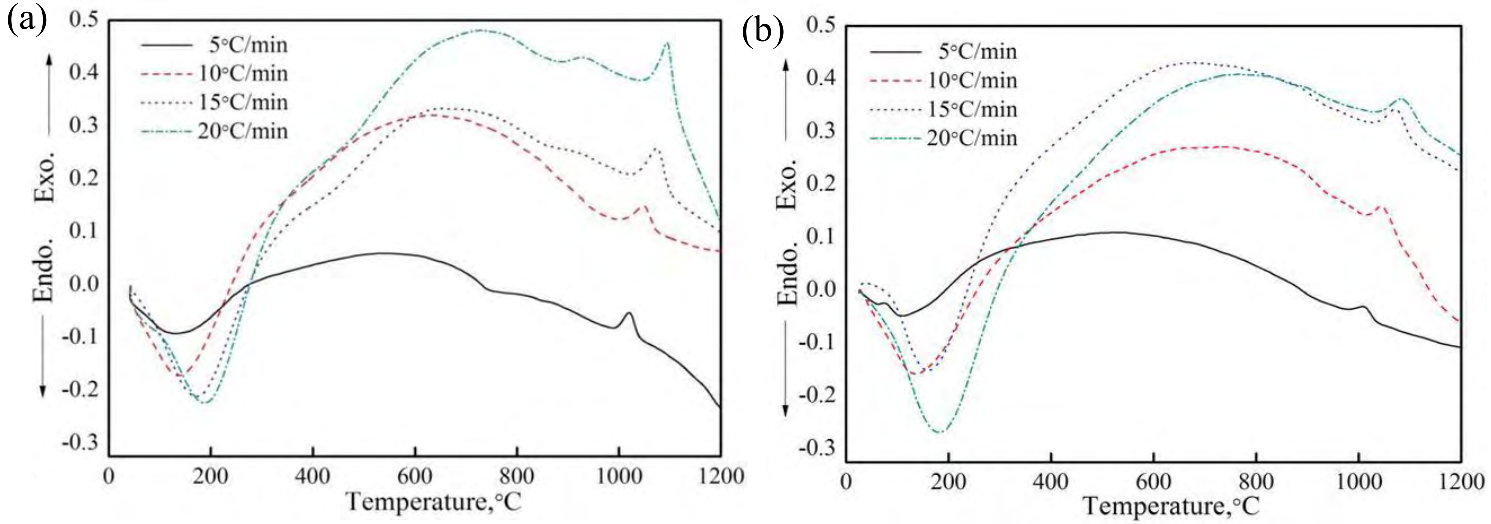


DTA curves of (a) KGP and (b) rGO/KGP at different heating rates

Summary of the crystallization kinetics parameters of the KGP and rGO/KGP

| Sample | Heating rate (°C/min) | Crystallization peak $Tp$(°C) | $\Delta T$ | $n$ | Activation energy (kJ/mol) | Average value $n$ |
|---|---|---|---|---|---|---|
| KGP | 5 | 1020 | 25 | 5.32 | 248 | 4.4 |
| | 10 | 1049 | 35 | 4.29 | | |
| | 15 | 1075 | 38 | 4.06 | | |
| | 20 | 1095 | 40 | 3.95 | | |
| rGO/KGP | 5 | 1011 | 33 | 4.31 | 240 | 3.5 |
| | 10 | 1048 | 45 | 3.30 | | |
| | 15 | 1073 | 45 | 3.52 | | |
| | 20 | 1086 | 55 | 2.85 | | |

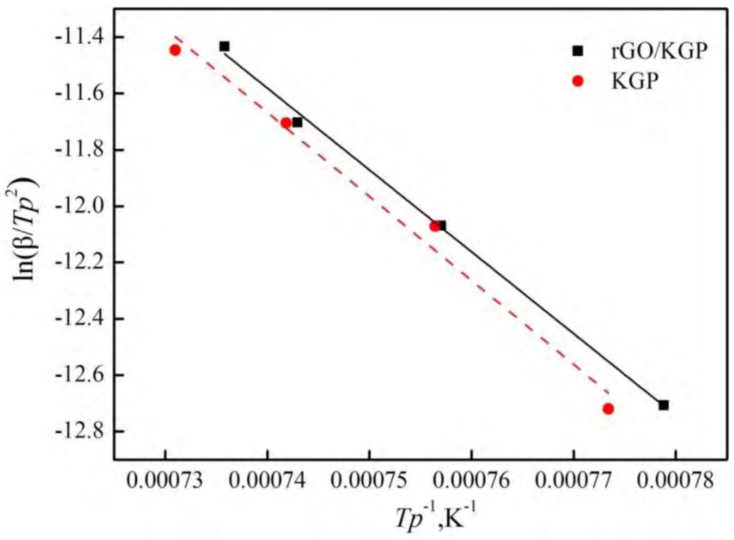


Kissinger plots of the KGP and rGO/KGP

# 5. Thermal evolution of rGO/KGP

## 5.2 Phase composition and microstructure

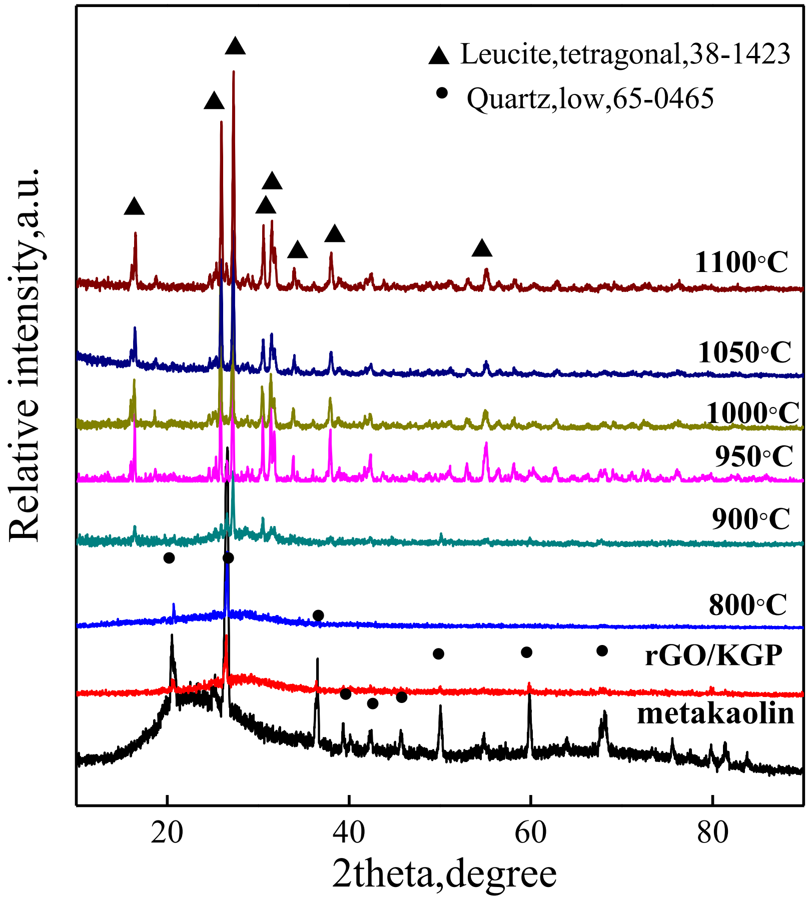


XRD patterns of rGO/KGP composites after high temperature treatment at different temperatures

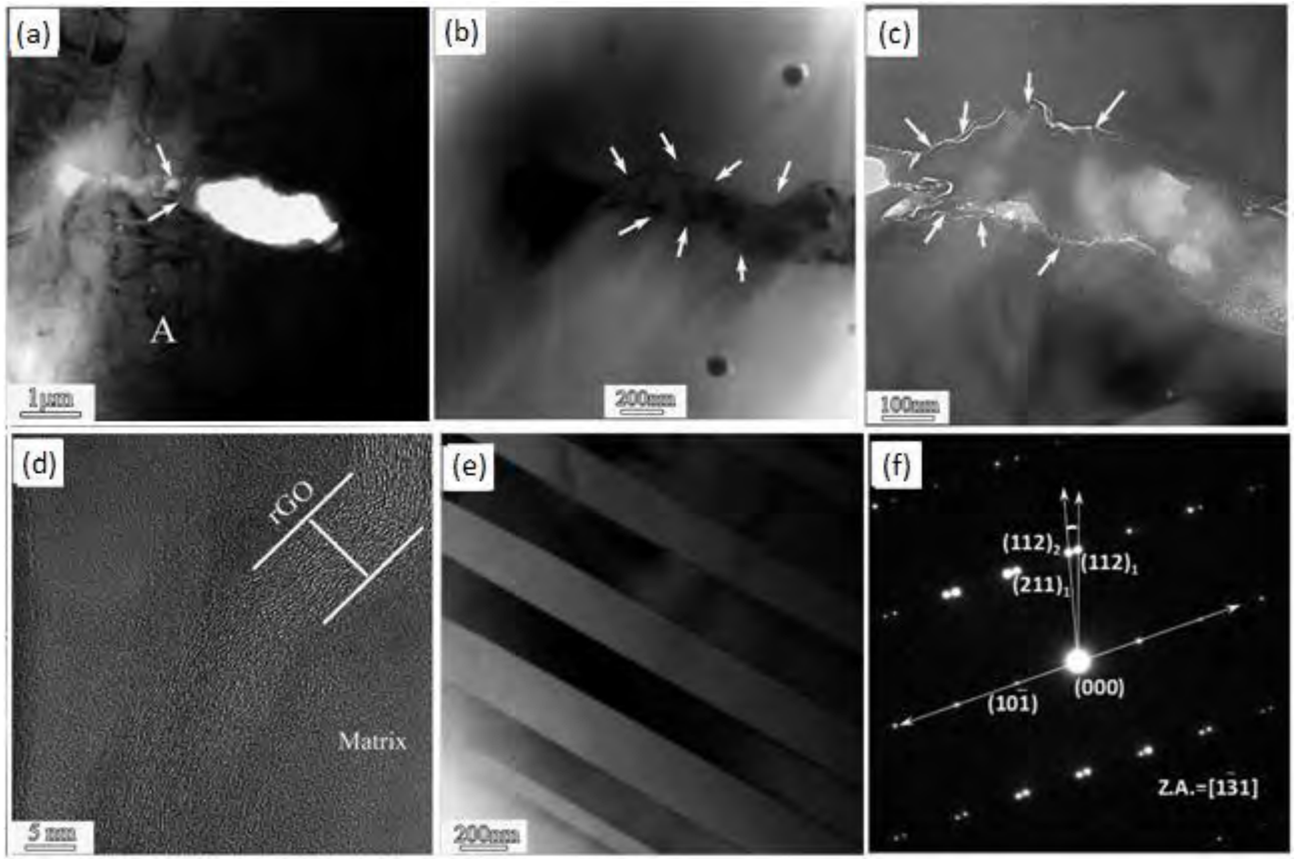


TEM images of the rGO/KGP1000 sample: (a) low magnification, (b) HAADF STEM image, (c) high magnification, (d) HRTEM of rGO and geopolymeric matrix, (e) high magnification of the matrix, (f) SAD pattern of area A

# 5. Thermal evolution of rGO/KGP

## 5.2 Phase composition and microstructure

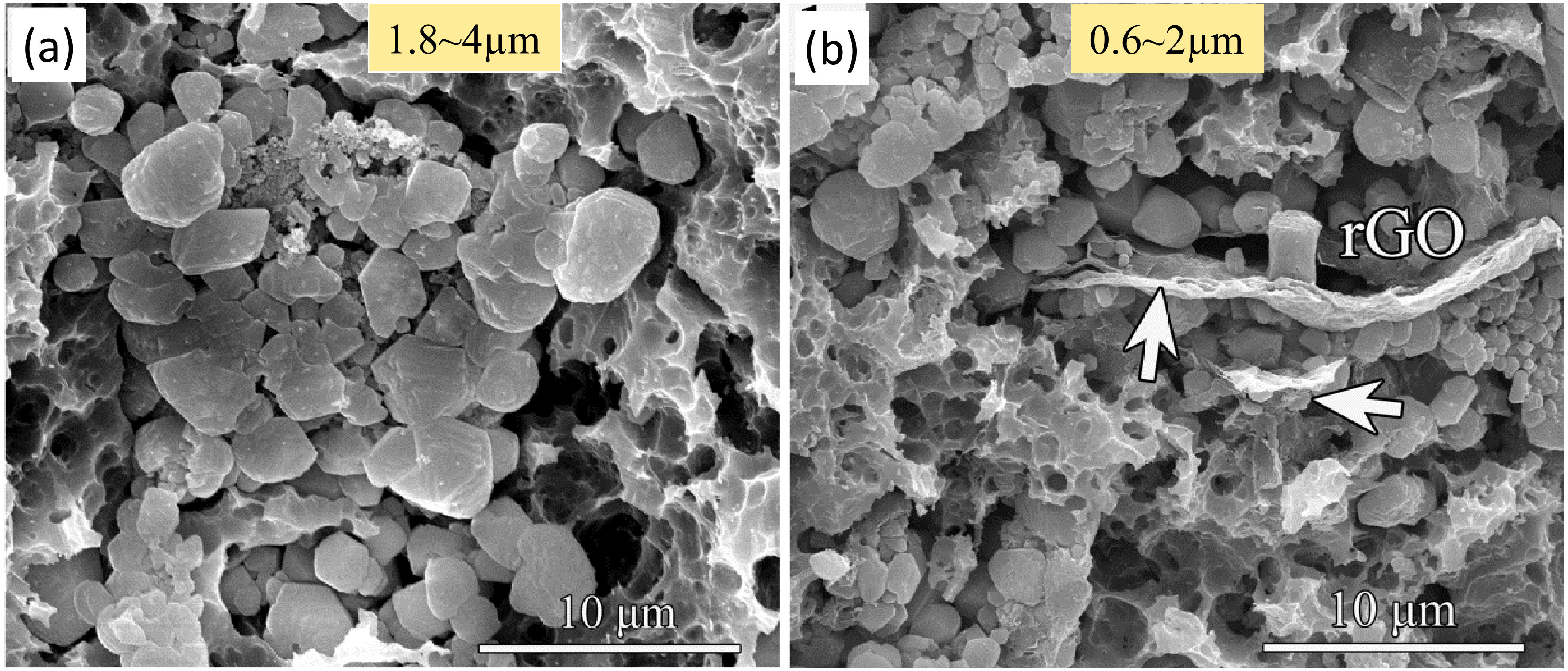


SEM images of (a) KGP1000 and (b) rGO/KGP1000
(etching in 3 wt% HF for 30s )

# 5. Thermal evolution of rGO/KGP

## 5.3 Fracture morphology

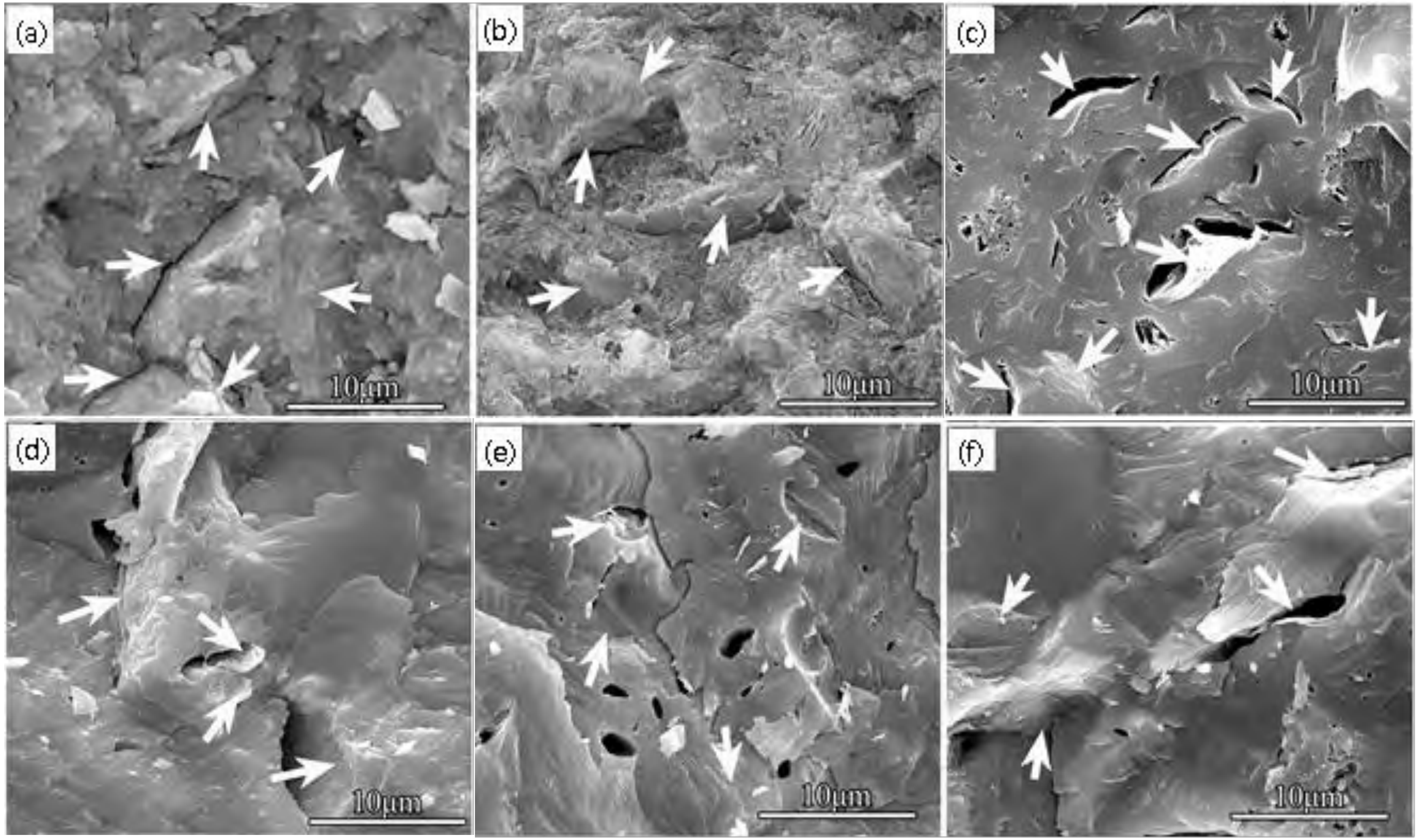


Typical microstructure of fracture surface of rGO/KGP composites after high temperature treatment:
(a) rGO/KGP, (b) rGO/KGP800, (c) rGO/KGP900, (d) rGO/KGP1000, (e) rGO/KGP1050, (f) rGO/KGP1100

# 5. Thermal evolution of rGO/KGP

## 5.3 Fracture morphology

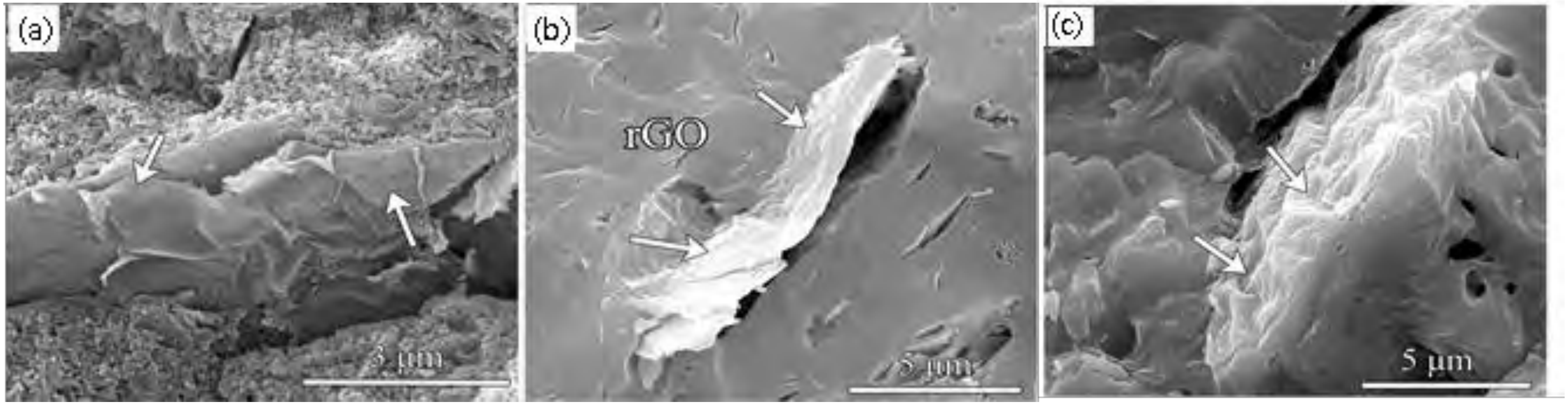


High magnification SEM images of fracture surface morphologies of rGO/KGP composites after high temperature treatment: (a) rGO/KGP800, (b) rGO/KGP900, (c) rGO/KGP1000

# 5. Thermal evolution of rGO/KGP

## 5.4 Mechanical properties

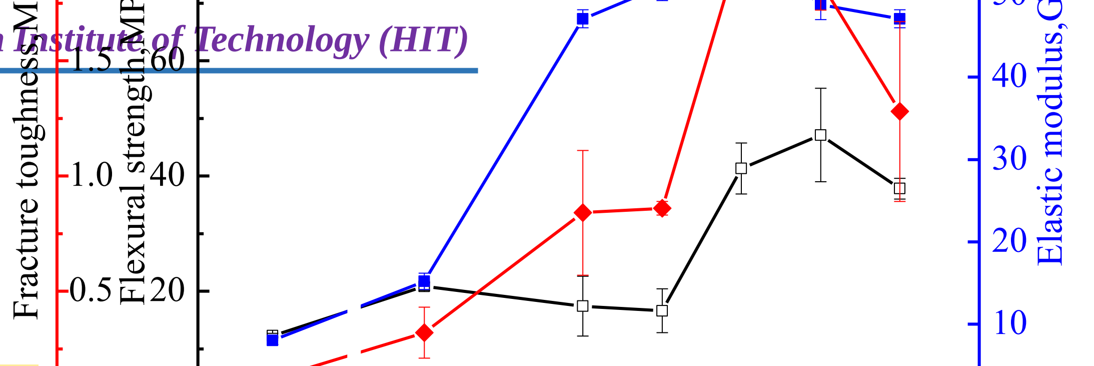

2.01Pa·m$^{1/2}$/41.3 Mpa/56.3GPa

2.04Pa·m$^{1/2}$/91.1 Mpa/60.5GPa

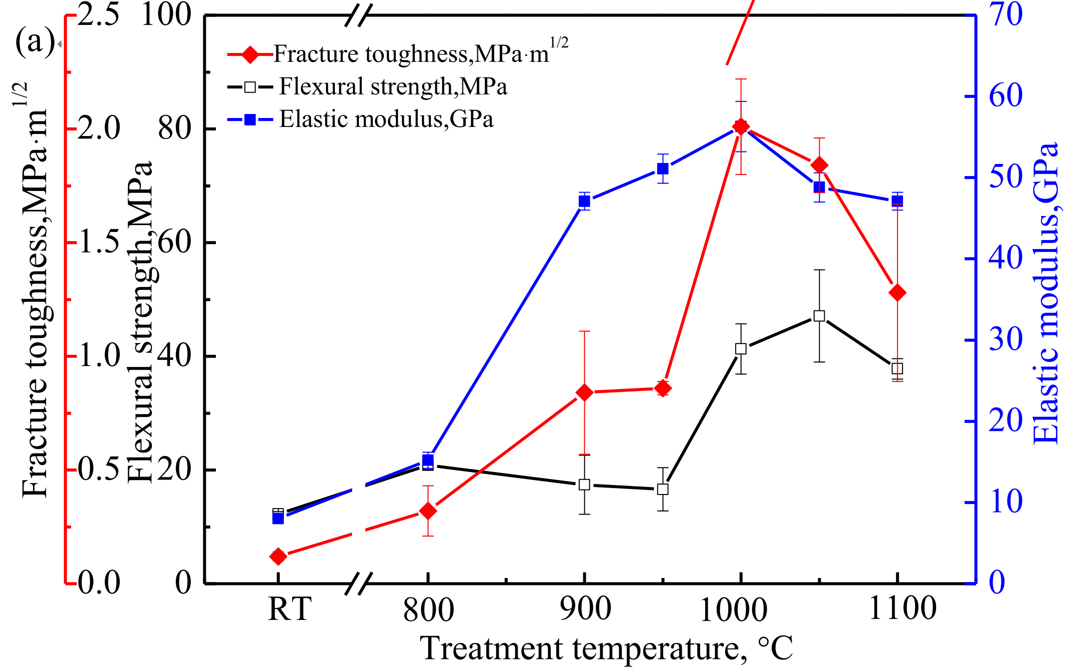


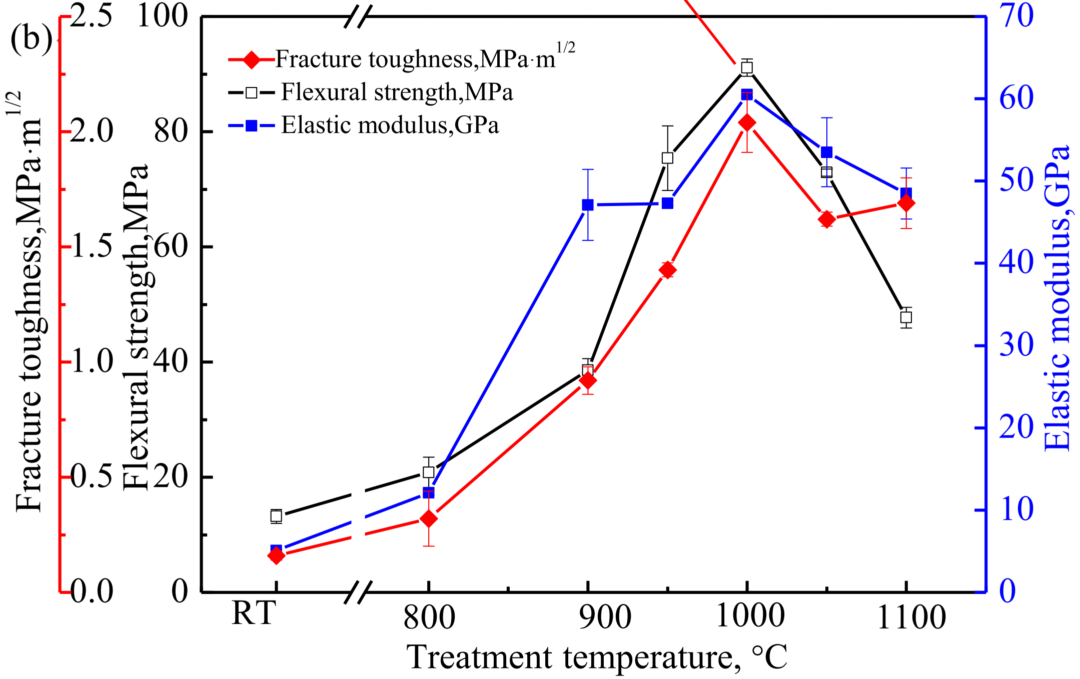


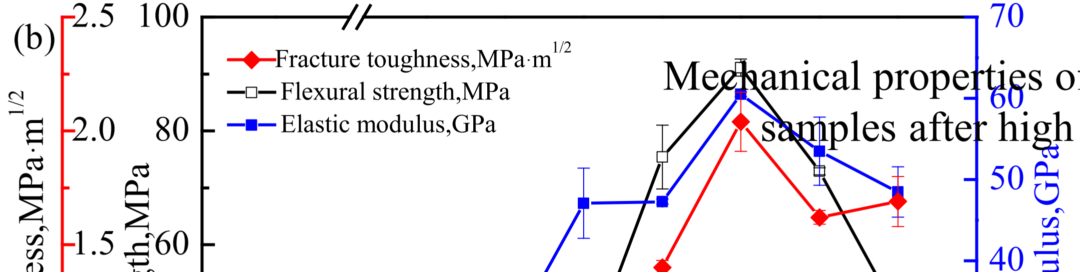

Mechanical properties of (a) KGP and (b) rGO/KGP samples after high temperature treatment

# 6. Conclusions

- GO is easily reduced in situ under alkaline conditions, and exhibits long-term stability and well dispersion in the geopolymeric solution. *In-situ* reduction occurs as a consequence of reducing/eliminating C=O and C–O bonds. Meanwhile, The reduction degree of rGO increased with the increasing temperatures. The C/O ratio increased from 2.48 (GO) to 3.36 (rGO, 80$^{o}$C) with the elevated temperatures.

- The introduction of GO has no obvious effects on the global structure of amorphous geopolymer matrices, and following reduction, the rGO sheets which dispersed homogeneously in the geopolymer matrix showed well bonding state to the matrix, resulting in the improvement of mechanical properties.

# 6. Conclusions

- rGO/KGP could fully transform to rGO/leucite composites after heat treatment at 1000$^{o}$C for 30 min. The presence of rGO in KGP matrix leads to the refinement of leucite grains but has no obvious effect on the lattice parameters of leucite. rGO sheets with scrolled and fold features disperse homogeneously in the leucite matrix, showing no interface reaction between rGO and matrix.

- Much more remarkable improvement in mechanical properties was achieved due to the introduction of rGO sheets into the matrix. The high-temperature treatment significantly improves the hardness of both rGO/KGP and pure KGP. Compared with those of the leucite sample (KGP1000), the mechanical properties of rGO/leucite (rGO/KGP1000) reach their own peak values, respectively, indicating the significant strengthening and toughening effect from graphene.

# Institute for Advanced Ceramics (IAC)

**Institute for Advanced Ceramics,**
**School of Materials Science and Engineering,**
**Harbin Institute of Technology**

**Pro. Dechang Jia**

**Ph.D Peigang He**

**Ph.D Jingkun Yuan**

Yikuang Str No2, Science Park of HIT, C3 Building, Room 516
Zip Code：150080
Fax: +86-451-86414291;
Tel: +86-451-86418792

# Thank You for Your Attention

# *Welcome to HIT*


Weihai Harbin Shenzhen